Acta Chemica Scandinavica, 1994: 48: 815–822
Printed in Belgium – all rights reserved

ACTA
CHEMICA SCANDINAVICA
ISSN 0904–213X

The Crystal Structure of I_2O_4 and its Relations to Other Iodine–Oxygen-Containing Compounds

Helmer Fjellvåg and Arne Kjekshus†

Department of Chemistry, University of Oslo, PO Box 1033, N-0315 Oslo, Norway

Fjellvåg, H. and Kjekshus, A., 1994. The Crystal Structure of I_2O_4 and its Relations to Other Iodine–Oxygen-Containing Compounds. – Acta Chem. Scand. 48: 815–822 © Acta Chemica Scandinavica 1994.

Although the existence of iodine dioxide (I_2O_4) has been known since 1844, its crystal structure has remained unsolved up to the present. The main reason for this is that I_2O_4 is obtained as a fine powder through controlled hydrolysis of $(IO)_2SO_4$ and that no suitable solvent for recrystallization of I_2O_4 has been found. The crystal structure of I_2O_4 has been determined from combined powder X-ray (synchrotron radiation, HASYLAB, DESY, Hamburg) and neutron (ILL, Grenoble) diffraction data. I_2O_4 crystallizes monoclinically [$a = 848.3(1)$, $b = 669.6(1)$, $c = 833.3(1)$ pm, $\beta = 124.69(1)°$; space group $P2_1/c$; all atoms in position $4e$]. The I_2O_4 structure is to a reasonable approximation a one-dimensional solid, comprising infinite ...–I–O–IO_2–O–... chains (in the listed order, tri- and penta-valent iodine), which are bonded together by much weaker interchain interactions. The atomic arrangement in I_2O_4 is discussed mainly in relation to the structures of $(IO)_2SO_4$ from which the dioxide is synthesized, and I_2O_5, into which it decomposes. Its relation to other iodine–oxygen-containing compounds is also considered.

Iodine oxides and oxoacids have been known and studied since the early days of chemistry. As time has passed, the focus of interest has shifted from the verification of their existence and stoichiometry, to structural characterization by increasingly sophisticated methods (cf. Refs. 1–6 and references therein). Although iodine dioxide (I_2O_4) was prepared by Millon[7] in 1844, its atomic arrangement remained unknown. The main reasons for this are that I_2O_4 is only obtained as a fine powder through controlled hydrolysis of $(IO)_2SO_4$, that no suitable solvent for recrystallization of I_2O_4 has been found, and that I_2O_4 decomposes (to I_2O_5 and I_2) at such a low temperature (below 150–200 °C) that a thermal means of increasing the crystal size is excluded (cf. Ref. 1 and references therein).

Hence, one must rely upon powder diffraction data in order to solve the crystal structure of I_2O_4. Iodine and oxygen have a large difference in scattering power for X-rays, whereas they have about equal scattering lengths for neutrons. The determination of the I_2O_4 crystal structure from either X-ray or neutron powder diffraction is accordingly a difficult task. The strategy to utilize a combination of powder X-ray and neutron diffraction data to attack this problem was consequently developed some 20 years ago. At our home base, several data sets of the best possible powder X-ray (Guinier–Hägg technique) and neutron (OPUS, two-axis diffractometer at the JEEP II reactor, Kjeller) diffraction data, were collected. However, despite all efforts the I_2O_4 crystal structure remained unsolved. Better experimental and computational facilities were required for solving the structure. By means of synchrotron radiation data (HASYLAB) the crystal structure of I_2O_4 is now solved (see also Ref. 8) and refined by high-resolution powder neutron diffraction data (ILL). In the present paper the atomic arrangement of I_2O_4 is discussed in relation to the crystal structures of $(IO)_2SO_4$,[5] from which I_2O_4 is synthesized, and I_2O_5,[3] which is the thermal decomposition product of I_2O_4. More briefly, the relationship to other iodine–oxygen-containing compounds is considered.

Experimental

I_2O_4 was prepared as described in Ref. 1 by controlled hydrolysis of $(IO)_2SO_4$ according to the reaction:

$$4(IO)_2SO_4(s) + 4H_2O(g) \rightarrow 3I_2O_4(s) + I_2(s/g) + 4H_2SO_4(l)$$

Most of the evolved H_2SO_4 was naturally drained away during the hydrolysis carried out on a plate of porous porcelain. The remaining H_2SO_4 and I_2 were removed by careful washing with absolute ethanol. The final product of I_2O_4 was dried in a vacuum desiccator.

† To whom correspondence should be addressed.

Polycrystalline samples of I_2O_5 were obtained from *p.a.* grade (di)iodine pentoxide (Merck) by heat treatment at 250 °C. Owing to the highly hygroscopic nature of I_2O_5 the samples were kept in sealed glass capsules between (and in some cases during) the experiments.

The purity and homogeneity of the I_2O_4 and I_2O_5 samples were checked by room temperature, powder X-ray diffraction (PXD; Guinier technique, Cu$K\alpha_1$ radiation, Si as internal standard) and differential scanning calorimetry (DSC) measurements (Mettler TA 3000 system, 100 mg sample, heating rate 5 K min^{-1}). All PXD reflections are accounted for by indexing, and the derived unit-cell dimensions are consistent with those reported in Refs. 2 and 4.

High-temperature PXD was performed at temperatures between 293 K and the decomposition of I_2O_4 (in I_2O_5 and I_2) and I_2O_5 (in I_2 and O_2) using a Guinier–Simon camera (Enraf–Nonius) and Cu$K\alpha_1$ radiation. The samples were placed in sealed quartz capillaries and heated at a rate of 30 K h^{-1}.

For the solving of the I_2O_4 crystal structure and the refinements of the I_2O_4 and I_2O_5 crystal structures, various sets of powder diffraction data were collected: (i) Guinier data (I_2O_4 and I_2O_5) taken with Cu$K\alpha_1$ radiation ($\lambda = 154.0598$ pm) for $5 < 2\Theta < 54°$ at Department of Chemistry, University of Oslo (UO). Integrated intensities were derived using a Nicolet L 18 film-scanning system and the SCANPI[9] computer program. (ii) Synchrotron radiation data (I_2O_4) collected at HASYLAB, DESY, Hamburg, with $\lambda = 139.17$ pm for $8 < 2\Theta < 79.4°$ (a PSD covering 2.7° was moved in steps of $\Delta(2\Theta) = 1.7°$, counting time 1–2 min at each setting). For experimental details, see Ref. 8. (iii) Powder neutron diffraction (PND) data (I_2O_4 and I_2O_5) collected at the OPUS III diffractometer at the JEEP II reactor, IFE, Kjeller, using neutrons of wavelength 187.7 pm and a bank of 5 detectors placed 10° apart. Data were collected for $5 < 2\Theta < 100°$ in steps of $\Delta(2\Theta) = 0.05°$. (iv) PND data (I_2O_4) collected with the D1A diffractometer at ILL, Grenoble ($\lambda = 196.2$ pm) for $6 < 2\Theta < 135°$. The step length was $\Delta(2\Theta) = 0.05°$.

For details concerning the determination of the structure of I_2O_4 reference is made to Ref. 8. The Pawley[10] and Hewat[11] versions of the Rietveld[12] program were used in the least-squares refinements. The scattering factors for X-rays were taken from Ref. 13 and the neutron scattering lengths from Ref. 14.

Crystal data

I_2O_4. 317.804 g mol^{-1}. Irregular shaped yellow crystals of a few μm maximum size. Monoclinic, with $a = 848.3(1)$, $b = 669.6(1)$, $c = 833.3(1)$ pm, $\beta = 124.69(1)°$ (see also Refs. 2 and 8). Unit-cell volume: 389.15×10^6 pm^3. Observed density: 2.57 g cm^{-3} at 25.00 °C. Unit-cell content: 4 ($Z_{obs} = 3.89$) I_2O_4. (The discrepancy between the postulated and observed unit-cell content is attributed to the small particle size.) Systematic extinctions: $h0l$ absent when $l = 2n + 1$, $0k0$ absent when $k = 2n + 1$. [The verification of the latter extinction rule is somewhat uncertain owing to the few reflections accessible. Electron diffraction (TEM) and infrared and Raman spectroscopic[6] data are consistent with a centrosymmetric space group.] Space group: $P2_1/c$.

I_2O_5. Crystal data are given in Ref. 3, here quoting only: $a = 1103.6(3)$, $b = 506.3(1)$, $c = 813.5(2)$ pm, $\beta = 107.18(2)°$; $Z = 4$; $P2_1/c$.

Structure determination and refinements

The approximate positions of the two iodine atoms in the asymmetric unit of I_2O_4 were deduced from Patterson maps, based on F_o^2 values (347 of which 54 were rejected) derived through profile deconvolution of PXD (synchrotron) data. These iodine positions were nearly the same as found several years earlier from the integrated intensities on Guinier photographs. After refinement of the parameters for these atoms (using F_o^2 data), it became possible to derive reasonable oxygen positions from difference Fourier maps. The positional parameters and the isotropic temperature factors for all atoms [in position 4*e* of the space group $P2_1/c$] were then subjected to profile refinements on the basis of ILL PND data. An unsatisfactory R_n factor (about 60) was initially obtained before renewed difference Fourier maps [using different subsets of $F_o^2(hkl)$ data] indicated that one of the originally suggested oxygen atoms was wrong. The low values finally obtained for the reliability factors ($R_{profile} = 0.092$ and 0.051 for the HASYLAB and ILL data, respectively) leave no doubt that the I_2O_4 structure is correct. Refined positional parameters are listed in Table 1, and observed and difference profiles are shown in Fig. 1.

It is appropriate to recapitulate the important steps in the structure determination; Guinier data and synchrotron PXD data both provided the correct unit cell (through trial-and-error indexing and subsequent least-squares refinement), and both provided reasonable coordinates for the iodine atoms through Patterson maps. Synchrotron data with good resolution and good counting statistics, and also covering a wider $\sin\Theta/\lambda$ range, were required for the identification of the oxygen atoms by difference Fourier maps. PND data were finally required for the verification of the suggested locations of the oxygen atoms. Since oxygen scatter neutrons equally well as iodine, the best atomic coordinates for the oxygen atoms are those obtained from profile refinement of PND data. The best set of positional parameters are undoubtedly those derived from ILL data, and this selection is emphasized by italics in Table 1.

After the crystal structure of I_2O_4 was solved, an interesting question was: How reliable positional parameters can be obtained from PND and PXD data of lower

Table 1. Positional parameters (with calculated standard deviations) for the crystal structure of I_2O_4 as derived from different sets of powder diffraction data. All atoms in position 4*e*; $\pm(x, y, z; x, 1/2-y, 1/2+z)$; space group $P2_1/c$. Recommended set of parameters (ILL) are printed in italics.

		PXD		PND	
		Guinier, UO	Synchroton HASYLAB	IFE	ILL
Atom	Parameter	Integrated intensity	Profile	Profile	Profile
I(1)	*x*	0.684(1)	0.6813(4)	0.6800(10)	*0.6780(6)*
	y	0.245(1)	0.2440(5)	0.2471(10)	*0.2427(9)*
	z	0.327(1)	0.3253(4)	0.3249(10)	*0.3222(6)*
I(2)	x	0.145(1)	0.1392(4)	0.1420(8)	*0.1417(6)*
	y	0.372(1)	0.3697(4)	0.3721(9)	*0.3738(7)*
	z	0.328(1)	0.3225(4)	0.3244(9)	*0.3221(7)*
O(1)	*x*	0.297(10)	0.3003(31)	0.3126(9)	*0.3123(6)*
	y	0.046(10)	0.0261(40)	0.0482(11)	*0.0473(7)*
	z	0.739(11)	0.7599(31)	0.7537(8)	*0.7506(5)*
O(2)	*x*	0.283(10)	0.2889(29)	0.3044(11)	*0.3087(7)*
	y	0.053(11)	0.0432(40)	0.0540(11)	*0.0497(7)*
	z	0.082(10)	0.0698(30)	0.0953(9)	*0.0925(6)*
O(3)	*x*	0.667(10)	0.6692(22)	0.6729(10)	*0.6780(6)*
	y	0.145(11)	0.1705(27)	0.1503(8)	*0.1493(6)*
	z	0.527(10)	0.5098(24)	0.5199(10)	*0.5244(6)*
O(4)	*x*	0.913(10)	0.9397(27)	0.9474(10)	*0.9409(5)*
	y	0.224(11)	0.2466(43)	0.2422(10)	*0.2430(8)*
	z	0.993(10)	0.9519(28)	0.9507(7)	*0.9511(6)*
R		0.12 integrated intensity	0.0092 profile	0.062 nuclear	0.051 profile

quality? The ILL positional parameters served as inputs in these refinements, and the resulting values from IFE PND and UO PXD data are juxtaposed in Table 1. A comparison shows that the parameters from the two PND studies are in good agreement. The mismatches for the PXD findings are larger, and concern mainly the positional parameters for the oxygen atoms.

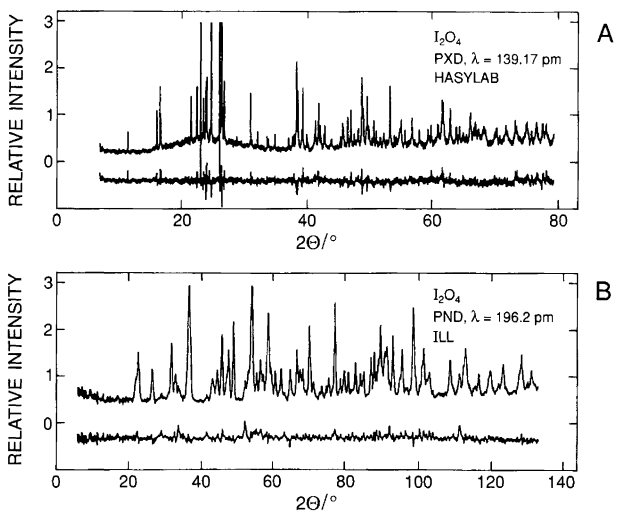

Fig. 1. Observed and difference (observed−calculated) (A) PXD and (B) PND profiles for I_2O_4 at 298 K for data collected at HASYLAB and ILL, respectively.

A corresponding refinement of the I_2O_5 structure[3] on the basis of IFE PND data gave the positional parameters listed in Table 2. Comparison of these findings with the single-crystal X-ray results show agreement within one standard deviation except for *x* and *z* for I(1) and *x* and *y* for O(3). According to the standard deviations, there is, as expected, a priority for the single-crystal data for the iodine atoms and for the PND data for the oxygen atoms. For principal reasons we will not mix results from different experiments, and in the following we will hold on to the single-crystal results.

Description and discussion of the I_2O_4 structure

Relevant interatomic distances and angles in the crystal structure of I_2O_4, as calculated from the unit-cell dimensions and the recommended set of positional parameters (ILL) in Table 1, are given in Table 3. A projection of the structure along [010] is shown in Fig. 2. The I_2O_4 structure may to a reasonable approximation be described as

Table 2. Positional parameters (with calculated standard deviations) for the crystal structure of I_2O_5 as derived from PND data [IFE; space group $P2_1/c$, all atoms in 4*e*, 192 reflections, $R_n = 0.083$). Corresponding values from single crystal X-ray diffraction data from Ref. 3 (printed in italics) are included for comparison.

Atom	*x*	*y*	*z*
I(1)	0.1278(9)	0.117(2)	0.217(2)
	0.1260(2)	*0.1143(6)*	*0.2136(3)*
I(2)	0.3737(9)	0.683(2)	0.159(1)
	0.3730(2)	*0.6825(5)*	*0.1597(3)*
O(1)	0.0127(7)	0.847(2)	0.152(1)
	0.015(3)	*0.850(7)*	*0.154(3)*
O(2)	0.1913(9)	0.035(2)	0.439(1)
	0.193(2)	*0.041(7)*	*0.434(3)*
O(3)	0.4944(9)	0.849(2)	0.332(2)
	0.486(2)	*0.862(6)*	*0.333(3)*
O(4)	0.3057(8)	0.500(2)	0.297(2)
	0.309(2)	*0.492(6)*	*0.300(3)*
O(5)	0.2492(9)	0.969(2)	0.112(2)
	0.250(2)	*0.968(6)*	*0.116(3)*

a one-dimensional solid, which comprises infinite ...–I–O–IO_2–O–... chains with intrachain I–O distances (marked by solid lines) between 177.6(7) and 215.0(5) pm. These chains are in turn linked together by

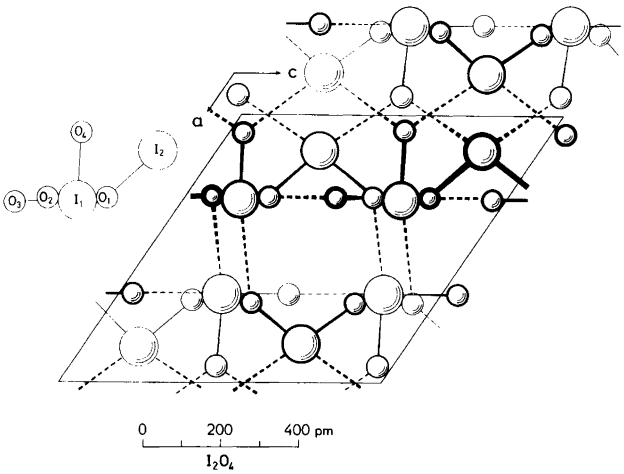

Fig. 2. The crystal structure of I_2O_4 projected along [010]. The numbering of the crystallographically non-equivalent atoms is shown on the left-hand side of the illustration. Broken lines designate weaker (secondary) I–O bonds [corresponding to I–O distances between 260.7(7) and 288.4(6) pm].

Table 3. Important interatomic distances (in pm, with calculated standard deviation) and angles (in °) in the crystal structure of I_2O_4.

Intramolecular distances:			
I(1)–O(3)	177.6(7)	I(2)–O(1)	192.4(9)
I(1)–O(4)	184.6(7)	I(2)–O(2)	193.4(5)
Intermolecular distances:			
I(1)–O(1)	205.4(6)		
I(1)–O(2)	215.0(5)		
I(1)–O(3)	260.7(7)	I(2)–O(4)	259.8(6)
I(1)–O(2)	288.4(6)	I(2)–O(4)	269.1(6)
Shortest distances neglected as bonding:			
I(1)–O(1)	313.6(7)	I(2)–O(4)	322.6(6)
I(1)–I(2)	346.5(7)	O(1)–O(3)	267.5(5)
Intra-intramolecular angles:			
O(1)–I(1)–O(2)	175.4	O(3)–I(1)–O(4)	97.1
O(1)–I(1)–O(3)	88.3	O(1)–I(2)–O(2)	95.8
O(1)–I(1)–O(4)	89.0	I(1)–O(1)–I(2)	121.1
O(2)–I(1)–O(3)	93.6	I(1)–O(2)–I(2)	119.6
O(2)–I(1)–O(4)	86.6		
Intra-intermolecular angles:			
O(1)–I(1)–O(2)	65.7	O(1)–I(2)–O(4)	80.5
O(1)–I(1)–O(3)	87.0	O(1)–I(2)–O(4)	174.0
O(2)–I(1)–O(2)	118.7	O(2)–I(2)–O(4)	79.3
O(2)–I(1)–O(3)	82.7	O(2)–I(2)–O(4)	173.1
O(2)–I(1)–O(3)	83.7	I(1)–O(2)–I(1)	112.2
O(2)–I(1)–O(3)	91.1	I(1)–O(2)–I(2)	117.6
O(2)–I(1)–O(4)	154.7	I(1)–O(3)–I(1)	143.2
O(3)–I(1)–O(3)	175.3	I(1)–O(4)–I(2)	114.0
		I(1)–O(4)–I(2)	129.7
Inter-intermolecular angles:			
O(2)–I(1)–O(3)	94.5	I(2)–O(4)–I(2)	116.2
O(4)–I(2)–O(4)	104.0		

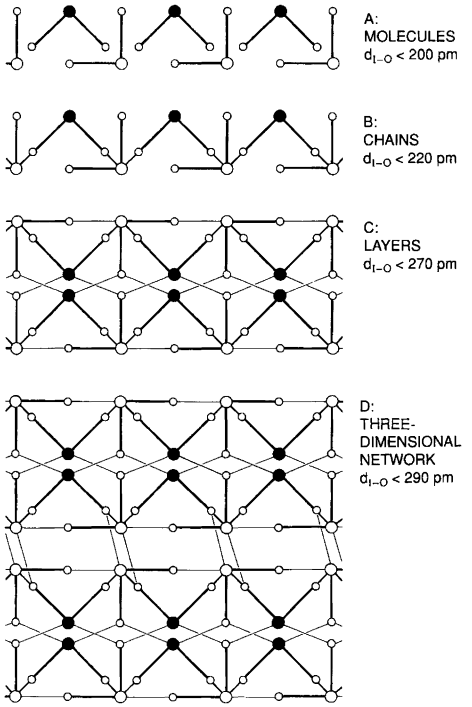

Fig. 3. Simplified and idealized representations of evolution stages for description of the I_2O_4 structure as more interatomic distances of increasing length are taken into account. Approximations A, B and C illustrate molecules, chains and layers and D symbolizes the fully developed three-dimensional network. Bonding interactions of decreasing strength are illustrated by decreasing line thickness. The open and filled larger circles represent I(1) (pentavalent) and I(2) (trivalent), respectively.

much longer interchain I–O distances [d_{I-O} = 260.7(7) to 288.4(6) pm] as shown by the broken lines in Fig. 2.

The grouping of the interatomic distances in the I_2O_4 structure in quite distinct categories (cf. Table 3) is indeed an interesting feature. It is very instructive to follow how the crystal structure image develops as more and more of the bonding interactions (with decreasing strength as d_{I-O} increases) are taken into account. As a starting point it is useful to simplify and idealize the I_2O_4 structure as shown in Fig. 3, and despite the stylized representation, the resemblance with the reality (Fig. 2) is quite striking. According to part A, where only $d_{I-O} < 200$ pm is included, the I_2O_4 structure can be seen as composed of two separate IO_2 molecules. When the distance limit is increased to $d_{I-O} < 220$ pm, the picture of the ...–I–O–IO_2–O–... chain approximation emerges in part B (cf. Fig. 2). On increasing the d_{I-O} limit, first to < 270 pm and then to < 290 pm, the appearance of the I_2O_4 structure again changes character. Part C mediates the impression of a layer structure approximation, whereas part D visualizes a fully developed three-dimensional network in the I_2O_4 structure.

From Table 3 and Figs. 2 and 3D (note the unlike representation of the different I–O interaction categories in the two illustrations) it is seen that I(1) and I(2), in total, take coordination numbers 6 and 4, respectively. The associated coordination polyhedra may be regarded as distorted octahedra and tetrahedra. On this basis it is natural to contemplate I(1) as penta-valent and I(2) as tri-valent, a conclusion which will be amplified below. [Already the chain approximation (Figs. 2 and 3B) indicates the valence situation in I_2O_4.]

A discussion of the interatomic distances in I_2O_4 in terms of the covalent bonding model might now seem appropriate. This could be made simple by partly repeating arguments from earlier considerations of the I_2O_5[3] and $(IO)_2SO_4$[5] structures. However, in this situation it seemed more productive to consider the bonding situation in I_2O_4 in relation to other iodine–oxygen-containing compounds in terms of the bond length versus bond valence concept (cf. Ref. 15 and references therein). Before entering this subject, more chemical relations between I_2O_4 and some of its closest relatives will be presented.

Figure 4 depicts the quasi-reversible $I_2O_5 \rightarrow (IO)_2SO_4 \rightarrow I_2O_4 \rightarrow I_2O_5$ cycle. The solid phases involved are illustrated by their crystal structures and the reactions by equations. The mechanism for the reaction between I_2O_5

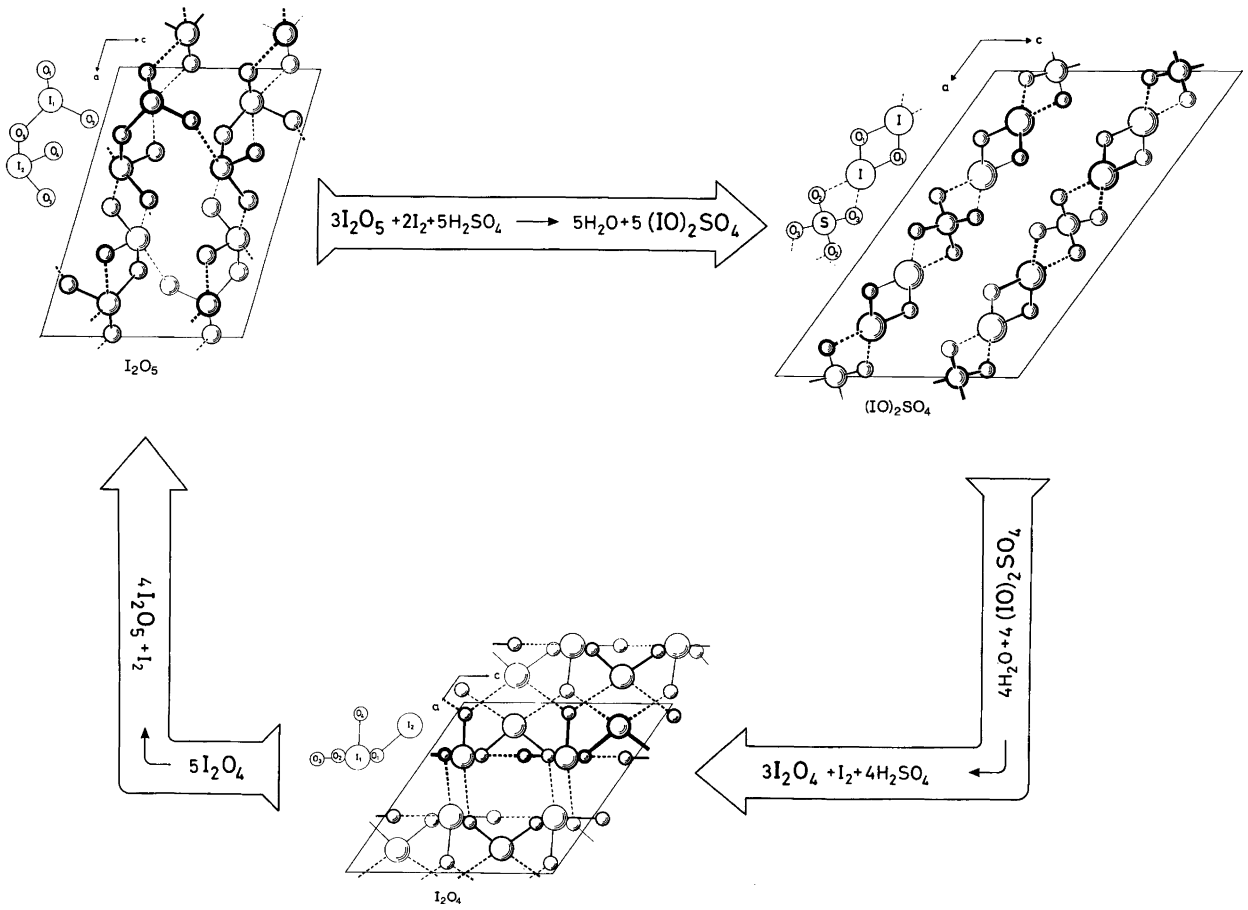

Fig. 4. The quasi-reversible $I_2O_5 \rightarrow (IO)_2SO_4 \rightarrow I_2O_4 \rightarrow I_2O_5$ cycle. Structure illustrations for I_2O_5 and $(IO)_2SO_4$ are taken from Refs. 3 and 5, respectively.

and I_2 in H_2SO_4 to give $(IO)_2SO_4$ is discussed in Ref. 16 and will not be repeated here.

The projection of the crystal structure of $(IO)_2SO_4$ on (001) in Fig. 5A justifies the simplification and idealization of the structure presented in the upper part of Fig. 5B. The middle section of Fig. 5B attempts to visualize how H_2O may be imagined to be incorporated into the $(IO)_2SO_4$ structure during the controlled hydrolysis (cf. Ref. 1) to form a hypothetic intermediate $(IO)_2SO_4 \cdot H_2O$ phase. The interactions between H_2O and SO_4 and I of the (bonafide) $(IO)_2SO_4$ structure may subsequently, after a slight atomic rearrangement and release of H_2SO_4(l) and I_2(s/g), be imagined to give I_2O_4 (as, e.g., visualized in the chain approximation, Fig. 4B and the lower part of Fig. 5B).

The thermally induced decomposition of I_2O_4 into I_2O_5 and I_2 takes place at 460 ± 10 K in a sealed capillary, cf. the unit-cell volume versus temperature data in Fig. 6. The reaction (see also Fig. 4) implies removal of 1/5 of the iodine atoms from the I_2O_4 structure. There is, unfortunately, no definite clue to decide as to whether I(1), I(2) or both are involved in the iodine elimination process. However, the linear thermal expansion coefficient perpendicular to c in the ac plane is significantly larger than those for b and c (in units of 10^{-5} K^{-1}: ~ 2.5 versus ~ 1.5 and ~ 2.0, respectively, whereas, owing to the significant influence of the variation in β, $\alpha_a \approx 0$ K^{-1}). For this reason it is tempting to postulate that neighbouring iodine atoms in the said direction are affected, and that for valence reasons, these ought to be the tri-valent I(2) atoms.

In order to visualize how the conversion process from I_2O_4 to I_2O_5 may take place, an extended version of the stylized layer representation in Fig. 3C is used as the starting point in the upper part of Fig. 7. (Remember that the chains are arranged lengthwise parallel to c.) Elimination of pairs of I(2) atoms and simultaneous rearrangement of bonds to form I_2O_5 'molecules' (going say from left to right in the illustration), the lower part of Fig. 7 is obtained. The significant feature of this purely hypothetic (molecular, since weak interactions are neglected) mechanism, is that precisely 1/5 of the iodine atoms are eliminated before a repeating unit is obtained. Although the essence of Fig. 7 is not utterly unfounded, the hypothetic aspect should be emphasized.

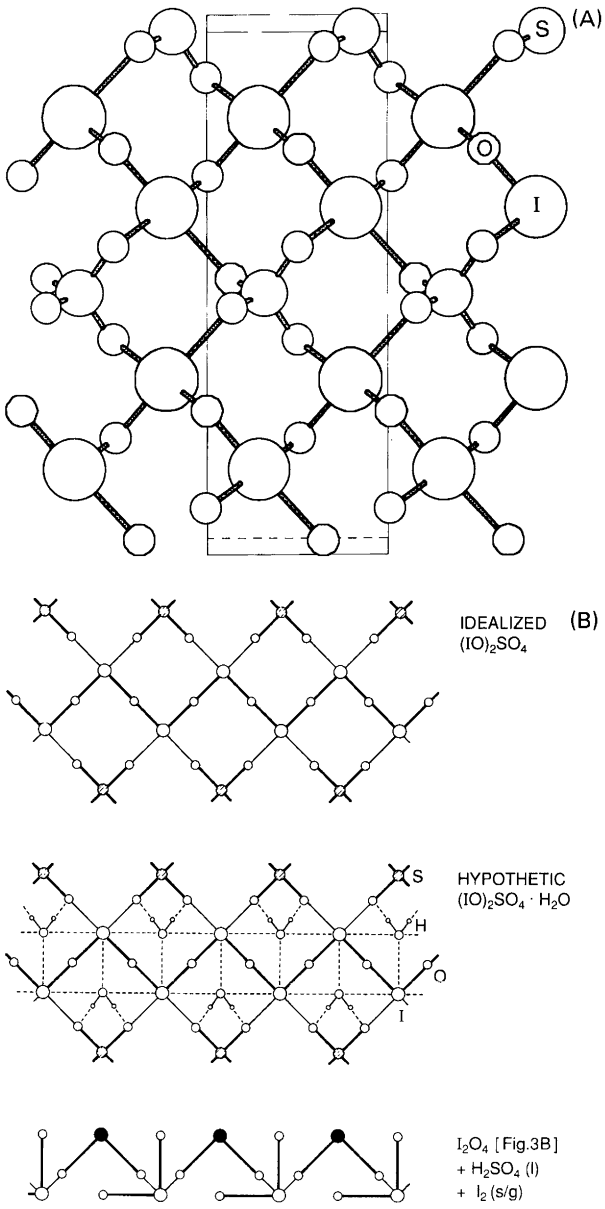

Fig. 5. (A) The crystal structure of $(IO)_2SO_4$ projected on (001). (B) Upper part: Simplified and idealized representation of the $(IO)_2SO_4$ structure in the same perspective as A. Middle part: The hypothetic $(IO)_2SO_4 \cdot H_2O$ phase. Lower part: Stylized I_2O_4 (quoted from Fig. 3B) as obtained after elimination of H_2SO_4(l) and I_2(s/g).

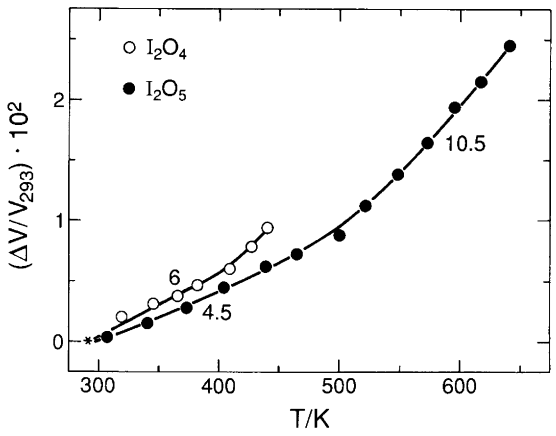

Fig. 6. Volume thermal expansion characteristics for I_2O_4 and I_2O_5. Expansion coefficients, $[\Delta V/(\Delta T V_{293})] \times 10^5$ K, are given on the illustration. Decomposition temperatures (note: in sealed capillaries): 460 ± 10 K for I_2O_4, 660 ± 10 K for I_2O_5. Calculated errors are about of the same size as symbols.

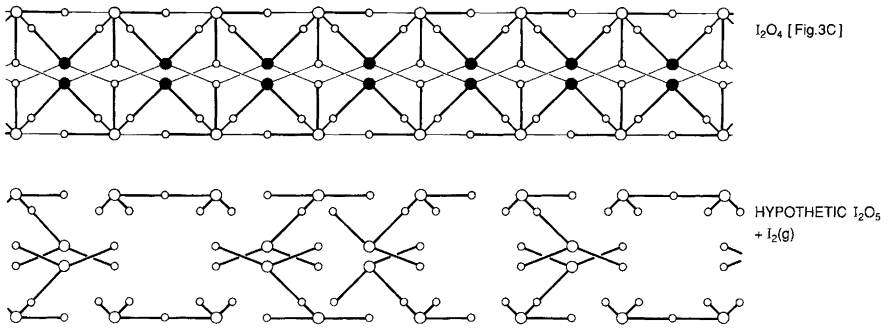

Fig. 7. Upper part: Layer version (quoted from Fig. 3C) of the stylized I_2O_4 structure. Lower part: Hypothetic I_2O_5 structure obtained after removal of 1/5 of iodine atoms from upper part and rearrangement of bonds.

Bond valences (V_i) have, according to Ref. 15, been calculated from the observed distances (d_{ij}/100 pm) according to the expression

$$V_i = \sum_j \exp\left[(D_{ij} - d_{ij})/b\right]$$

where D_{ij} is the bond valence parameter for the particular type of bond concerned and $b = 0.37$. For the compounds of current interest, Ref. 15 lists $D_{ij} = 2.00$, 1.93 and 1.624 for I^{V}–O, I^{VII}–O and S^{VI}–O, respectively. Based on the experience from the iodine–oxygen compounds in Table 4, it is suggested that D_{ij} is corrected to 1.98 for I^{V}–O and that $D_{ij} = 2.03$ is entered as representative for I^{III}–O. Using the latter values, one obtains $V_{I(1)-O} = 1.73 + 1.51 + 0.87 + 0.65 + 0.21 + 0.09 = 5.06$ and $V_{I(2)-O} = 1.33 + 1.30 + 0.21 + 0.17 = 3.01$ for the two different iodine atoms in I_2O_4. Three features appear worth mentioning. First, the firm conclusion that I(1) is pentavalent and I(2) is trivalent is unavoidable. Second, it is the number of bonds as well as their lengths which in sum carry the message about the valence for a given atom in a crystal structure. Judgements based on either of these two criteria alone may lead to incorrect conclusions. Third, it is quite remarkable that such a simple, empirical expression with few adjustable parameters is able to monitor the valence states in I_2O_4 with such an accuracy. The latter point is further strongly emphasized by the collection of bond valence data for related iodine–oxygen-containing compounds in Table 4.

It is worthwhile to note that the bond valence concept is not self-fulfilling in the sense that the choice of the parameter D_{ij} determines the valence for the atom considered. In fact, all the values for D_{ij} stated above would lead to the same conclusions about the iodine valences provided one is not too particular about the actual resulting numerical value for the valence. In other words, the number of bonds and their lengths carry the decisive information about the valence state, whereas the choice of D_{ij} merely determines the match between calculated and predicted V_i.

Table 4. Bond valence data for iodine–oxygen-containing compounds (see text).

	Bond valence						
Compound	Specification	Range	Sum	} Average	} Average	Ox-state	Ref.
$(IO)_2SO_4$	I–O	0.35–1.19	3.10			3	5
	S–O	1.42–1.48	5.80				6
I_2O_4	I(2)–O	0.17–1.33	3.01				
	I(1)–O	0.09–1.73	5.06		4.04	4	This work
$(IO_2)_3HSO_4$	I(5)–O	0.66–0.83	2.98				
	I(6)–O	0.73–0.79	3.04	3.01			
	I(1)–O	0.11–1.64	4.96				
	I(2)–O	0.11–1.74	4.89				
	I(3)–O	0.08–1.75	4.98				
	I(4)–O	0.08–1.74	4.86	4.92	4.28	13/3=4.33	
	S(1)–O	1.33–1.68	6.03				
	S(2)–O	1.29–1.67	6.04		6.04	6	17
I_2O_5	I(1)–O	0.08–1.79	5.15				
	I(2)–O	0.22–1.67	5.01		5.08	5	3
HI_3O_8	I(1)–O	0.14–1.73	4.89				
	I(2)–O	0.21–1.72	5.01				
	I(3)–O	0.22–1.65	4.90		4.93	5	18
HIO_3	I–O	0.12–1.72	5.16			5	19
H_5IO_6	I–O	1.05–1.50	7.09			7	20

References

1. Dæhlie, G. and Kjekshus, A. *Acta Chem. Scand. 18* (1964) 144.
2. Selte, K. and Kjekshus, A. *Acta Chem. Scand. 22* (1968) 3309.
3. Selte, K. and Kjekshus, A. *Acta Chem. Scand. 24* (1970) 1912.
4. Selte, K. and Kjekshus, A. *Acta Chem. Scand. 25* (1971) 751.
5. Furuseth, S., Selte, K., Hope, H., Kjekshus, A. and Klewe, B. *Acta Chem. Scand., Ser. A 28* (1974) 71.
6. Ellestad, O. H., Woldbæk, T., Kjekshus, A., Klæboe, P. and Selte, K. *Acta Chem. Scand., Ser. A 35* (1981) 155.
7. Millon, M. E. *Ann. Chim. Phys. 12* (1844) 345, 353; *J. Prakt. Chem. 34* (1845) 321, 337.
8. Lehmann, M. S., Christensen, A. N., Fjellvåg, H., Feidenhans'l, R. and Nielsen, M. *J. Appl. Crystallogr. 20* (1987) 123.
9. Werner, P.-E. Program SCANPI, Institute of Inorganic Chemistry, University of Stockholm, Sweden, 1981.
10. Pawley, G. S. *J. Appl. Crystallogr. 13* (1980) 630.
11. Hewat, A. W. The Rietveld Computer Program for the Profile Refinement of Neutron Diffraction Powder Patterns Modified for Anisotropic Thermal Vibrations, *UKAERE Harwell Report RRL 73/897* 1973.
12. Rietveld, H. M. *J. Appl. Crystallogr. 2* (1969) 65.
13. *International Tables for Crystallography*, Kynoch Press, Birmingham 1972.
14. Koester, L. and Rauch, H. IAEA Contract 2517/RB, IAEA, Vienna 1981.
15. Brese, N. E. and O'Keeffe, M. *Acta Crystallogr., Sect. B 47* (1991) 192.
16. Ahmed, M. A. K., Fjellvåg, H. and Kjekshus, A. *Acta Chem. Scand. 48* (1994) 537.
17. Rehr, A. and Jansen, M. *Z. Anorg. Allg. Chem. 608* (1992) 159.
18. Feikema, Y. D. and Vos, A. *Acta Crystallogr. 20* (1966) 769.
19. Garrett, B. S. *ORNL-1745*, Oak Ridge National Laboratory 1954.
20. Feikema, Y. D. *Acta Crystallogr. 20* (1966) 765.

Received March 22, 1994.